Acta Materialia 109 (2016) 151–161

Contents lists available at ScienceDirect

Acta Materialia

journal homepage: www.elsevier.com/locate/actamat

Full length article

On the origin of creep dislocations in a Ni-base, single-crystal superalloy: an ECCI, EBSD, and dislocation dynamics-based study

Farangis Ram [a, *], Zhuangming Li [a], Stefan Zaefferer [a], Seyed Masood Hafez Haghighat [a], Zailing Zhu [b], Dierk Raabe [a], Roger C. Reed [b]

[a] Max-Planck Institut für Eisenforschung GmbH, Max-Planck-str. 1, 40237, Düsseldorf, Germany
[b] Department of Materials, University of Oxford, Parks Road, Oxford OX1 3PH, UK

ARTICLE INFO

Article history:
Received 29 August 2015
Received in revised form
13 February 2016
Accepted 18 February 2016
Available online xxx

Keywords:
Single-crystal, Ni-base supperalloys
Creep dislocations
Dislocation dynamics
Low-angle grain boundaries

ABSTRACT

This work investigates the origin of creep dislocations in a Ni-base, single crystal superalloy subject to creep at an intermediate stress and temperature. Employing high angular resolution electron backscatter diffraction (HR-EBSD), electron channeling contrast imaging under controlled diffraction conditions (cECCI) and discrete dislocation dynamics (DDD) modelling, it is shown that low-angle boundaries—-which correspond to dendrite boundaries or their residues after annealing—are not the major sources of creep dislocations. At the onset of creep deformation, they are the only active sources. Creep dislocations are emitted from them and percolate into the dislocation-depleted crystal. However, the percolation is very slow. As creep deformation proceeds, before the boundary-originated dislocations move further than a few micrometers away from their source boundary, individual dislocations that are spread throughout the undeformed microstructure become active and emit avalanches of creep dislocations in boundary-free regions, i.e. regions farther than a few micrometer away from boundaries. Upon their activation, the density of creep dislocations in boundary-free regions soars by two orders of magnitude; and the entire microstructure becomes deluged with creep dislocations. The total area of boundary-free regions is several times the total area of regions covered by boundary-originated creep dislocations. Therefore, the main sources of creep dislocations are not low-angle boundaries but individual, isolated dislocations in boundary-free regions.

1. Introduction

Nickel-base superalloys are employed in high-temperature applications, particularly for jet propulsion and power conversion. To increase creep resistance, these alloys are produced as single crystals. Single-crystal superalloys are often fabricated by directional solidification techniques using competitive dendrite growth [1,2]. Casting is usually followed by a solution and ageing heat-treatment to achieve the desired microstructure [3,4] consisting of about 70% volume fraction of cuboidal γ′ precipitates coherently embedded in a solid solution γ matrix.

The as-processed γ/γ′ microstructure is dislocation-depleted. As creep-deformation proceeds, the microstructure becomes increasingly populated with creep dislocations [5–10]. In tertiary creep regime, characterized by a monotonically increasing strain rate, it has been suggested that sources of creep dislocations are the so-called grown-in networks of dislocations [11–14]. These networks, which are casting defects and which withstand the subsequent heat-treatment, are in fact low-angle grain boundaries.

It has been shown that the as-processed single crystals are not truly monocrystalline: low-angle boundaries exist, which accommodate lattice rotations of below 1° [15–19]. Instances of dislocation percolation from a boundary to dislocation-depleted crystal portions in the close vicinity of the grown-in low angle grain boundaries—a few micrometers—have been observed in TEM foils [11–14]. It has been suggested that: the boundary-generated dislocation loop segments are driven into the narrow γ channels by a shear stress, which results from the superposition of the applied stress and the misfit stress; during glide in the γ channels, the permeating dislocations deposit segments at the γ/γ′ interfaces [4]; these dislocations partially relieve the γ/γ′ misfit stress; and the gliding dislocations originated from different boundaries

* Corresponding author. Materials Science and Engineering Department, Carnegie Mellon University, 5000 Forbes Avenue, Pittsburgh, 15213-3890, PA, USA.
E-mail address: fram@cmu.edu (F. Ram).

http://dx.doi.org/10.1016/j.actamat.2016.02.038
1359-6454/

eventually meet, react, and result in dislocation networks [11,13,20].

The research reported in this paper was carried out to revisit the sources of creep dislocations by examining the evolution of dislocation density throughout the microstructure. A Re-containing Ni-base, single-crystal superalloy was studied to elucidate the microstructural evolution that control the early stages of creep deformation. Electron channeling contrast imaging (ECCI) and electron backscatter diffraction (EBSD) techniques were employed for microstructure characterization; and discrete dislocation dynamics (DDD) modelling was utilized for simulating the microstructural evolutions.

2. Materials and methods

The single-crystal superalloy studied here was prepared in the form of cylindrical bars of 10 mm diameter and 160 mm length using investment casting. Its chemical composition, Ni–8Cr–10Co–1.6Re–8.5W–5.8Al–8.5Ta in weight percent, was chosen consistent with the alloy design results of [21]. An industrial-scale investment casting facility was used for casting with a withdrawal speed of 229 mm/h, a mould temperature of 1540° C and a vacuum of better than 10^{-4} Pa. After casting, the single-crystal bars were carefully removed from the mould, sand blasted, macro-etched using an HCl + 5–10 vol.% H_2O_2 solution, and subjected to X-ray analysis using the back-reflection Laue technique to confirm their <001> orientation. Solution treatment was then carried out at 1305° C for 6 h followed by a two-step heat-treatment at 1120° C for 3 h and at 870 °C for 16 h. Tensile testpieces of 20 mm gauge length and 4 mm diameter were then machined from the fully heat-treated single-crystal bars such that their long axes were parallel to the growth direction of the single crystal, which is a <001> crystallographic direction. A schematic is shown in Fig. 1 a.

The tensile testpieces were subsequently subjected to a constant-load creep test at 900 °C up to rupture. Within the gauge section, the applied stress was uniaxial tensile of 450 MPa. The creep curve, displayed in Fig. 1 b, indicates a tertiary creep regime identified by the monotonic increase of strain rate with strain [4]. Rupture occurred at 22.1% strain after 194 h. The investigations reported in this paper were performed on the ruptured testpiece and were confined to a region of the testpiece close to the extensometer lips, where the accumulated local strain was estimated to be less than 0.1%.

The microstructure was examined using ECCI [22–24] and EBSD [25] in a Scanning Electron Microscope (SEM). ECCI was performed using a Zeiss Merlin scanning electron microscope (Carl Zeiss SMT AG, Germany) with a Gemini-type field emission gun electron column. The microscope was operated at 30 kV accelerating voltage and 2–5 nA probe current. The specimen was placed at 6 mm working distance and was tilted to an angle in the range [−4°,20°]. To observe dislocations, the ECCI under controlled diffraction conditions (cECCI) method [23] was employed. The computer program TOCA [26,27] was used for selection of suitable diffraction conditions from simulated electron channeling pattern (ECP).

EBSD measurements were carried out in a JEOL 6500F FEG scanning electron microscope operating at 15 kV accelerating voltage and high beam current mode and equipped with a Digiview 5 camera and the EDAX/TSL OIM DC software (version 7.0; EDAX/TSL, Draper, UT, USA). Patterns were captured with 2 × 2 binning on the camera, minimum camera gain, no averaging, no background removal, and no image processing. The recorded patterns were of 468 × 468 dimensionality with 12 bit depth. Beam scanning was performed in 1 μm or 2 μm steps.

Crystal orientation maps were measured using the EDAX/TSL

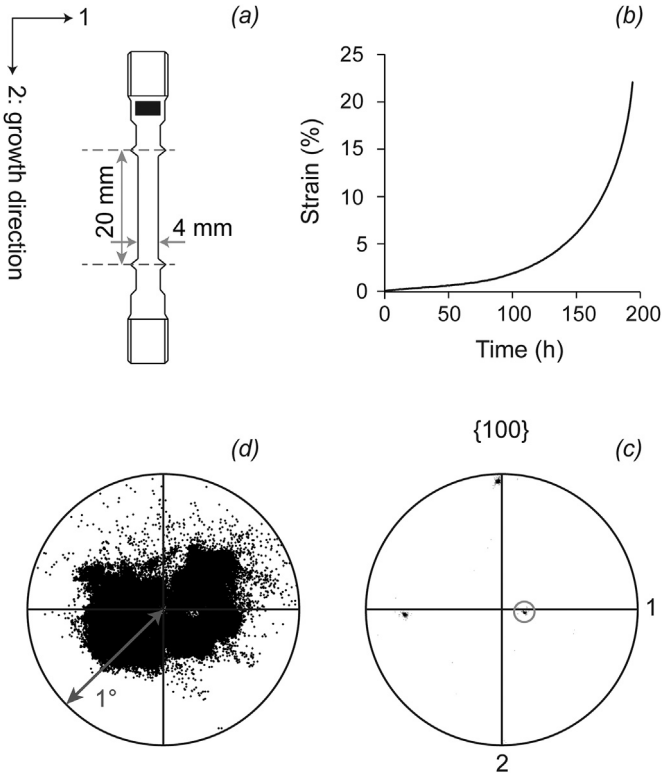

Fig. 1. (a) Schematic illustration of the examined testpiece before the creep test. The black rectangle marks the region that contains the EBSD-mapped areas. (b) The creep curve showing the engineering strain versus time at 900 °C and 450 MPa. (c) EBSD-based {100}-pole figure in stereographic projection of a region in the uncrept area. (d) The pole encircled in (c) is magnified by rotating it to the center of the pole figure and setting the maximum polar angle to 1°.

OIM DC software. The Kikuchi bands utilized for orientation derivation were detected using the classical two-dimensional Hough transform (2-D HT)-based algorithm [28,29]. Patterns were binned to 468 × 468 prior to applying the 2-D HT; 160 × 160 was set for Hough space resolution; a $\Delta\theta = 0.5^{\circ}$ pixels convolution mask was applied; and maximum 12 Kikuchi bands were used for orientation derivation.

Crystal rotations relative to a reference point on the map were obtained by applying the HR-EBSD method [30,31]. The density of geometrically necessary dislocations (GND) was computed using the HR-EBSD-based lattice curvature [32–34]. With a cubic symmetry, the three elastic stiffness constants at room temperature were assumed to be equal to the ones of CMSX-4, i.e. 13 × 13 MPa; $C_{11} = 243$ MPa; and $C_{12} = 153$ MPa [35]. The CrossCourt software v.3 (BLG Productions Ltd., UK) was used for lattice rotation and GND density calculations [30,32,36]. On each pattern, 28 regions of interests each of $C_{44} = 128$ pixels were considered.

To assess the evolution of dislocations during creep deformation, discrete dislocation dynamics (DDD) modelling was employed. DDD is well suited for the simulation of creep effects associated with dislocation mobility and their interactions based on the elasticity theory of dislocations [37–43]. For this study, the ParaDiS code was used [44]. A hybrid dislocation mobility rule with a climb/glide mobility ratio of 0.1 [38] was used to mimic climb-assisted mobility of dislocations along the γ/γ' interfaces at high temperature, i.e. ~900 °C. Isotropic elasticity with a shear modulus of 37 GPa and a Poisson ratio of 0.37 was assumed. The lattice parameter for the Ni alloy in the γ channels was taken as a = 0.36 nm, which leads to a <110> Burgers vector length of